PHYSICS-BASED CLASSIFICATION OF TARGETS IN SAR IMAGERY USING SUBAPERTURE SEQUENCES

Lawrence Carin, Gary Ybarra, Priya Bharadwaj, and Paul Runkle

Department of Electrical and Computer Engineering
Duke University
Durham, NC, 27708
lcarin@ee.duke.edu, runkle@ee.duke.edu

ABSTRACT

It is well known that radar scattering from an illuminated object is often highly aspect dependent. We have developed a multi-aspect target classification technique for SAR imagery that incorporates matching-pursuits feature extraction from each of a sequence of subaperture images, in conjunction with a hidden Markov model that explicitly incorporates the target-sensor motion represented by the image sequence. This approach exploits the aspect dependence of the signal features to facilitate maximum-likelihood identification. We consider SAR imagery containing targets concealed by foliage.

1. INTRODUCTION

The use of low-frequency, ultra wideband (UWB) imaging radar has recently been of interest for the detection and classification of tactical targets concealed by foliage [1,2]. The identification of such targets may be significantly enhanced by accounting for their anisotropic scattering behavior, *i.e.* the characteristics of the scattered signal may be highly variable with respect to the target-sensor orientation. An example of an object exhibiting such behavior is a flat plate. When the plate is illuminated from a direction close to normal incidence, or "broadside", a significant proportion of the incident energy is returned to the sensor. However, when illuminated away from normal incidence, the backscattered energy is significantly attenuated. When the radar is operating in a SAR mode, this anisotropic behavior will be manifested as a "flash" as the aperture passes the plate's broadside. In this paper we present an approach which exploits such anisotropic scattering to improve the detection and classification of tactical targets.

The present multi-aspect classification system is summarized in Figure 1. A SAR image of an unknown target at an unknown orientation is decomposed into a sequence of subaperture images corresponding to a sequence of target-sensor orientations. Recently [3] it has been shown that such subaperture images may be generated by applying directional filterbanks directly to the post-processed SAR image. A matching-pursuits [4] feature extraction is performed on each of the subaperture images to parameterize the salient directional information. Besides the directionally varying energy from broadside flashes, there may be other features in the scattered signal, such as aspect dependent resonances that may be exploited to improve the classification of tactical targets. This sequence of feature vectors may be thought of as a statistical sample of the directionally varying characteristics of the target. A framework which is well suited for describing such stochastic sequences is a hidden Markov model [5]. The sequence of multi-aspect feature vectors is used to train a continuous hidden Markov model for each target class. Maximum-likelihood target identification is then performed by associating a target under test with that model yielding the greatest conditional likelihood of the observation. With sufficient training from either physical models [6] or SAR imagery, this approach of combining physics-based features with the target-sensor geometry may provide significant gains in classification performance.

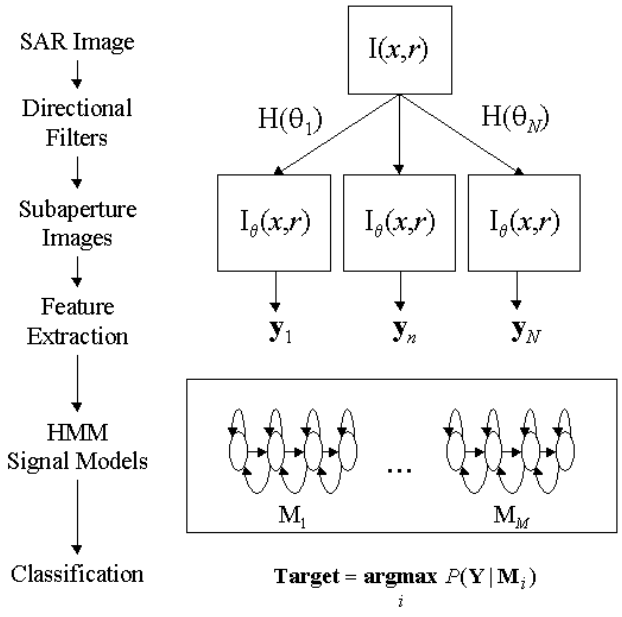

Figure 1. Block diagram of multi-aspect HMM SAR classification.

This paper is structured as follows. First, the directional filters used to create the subaperture images are reviewed. In Section 3 we discuss the matching-pursuits feature extraction applied to each image in the subaperture sequence. The incorporation of the target-sensor geometry into the hidden Markov model is addressed in Section 4. Results on the application of this

classification approach applied to SAR imagery containing tactical vehicles and clutter are presented in Section 5.

2. SUBAPERTURE IMAGE SEQUENCES

The exploitation of directionally dependent radar scattering for target identification requires that the target be illuminated by the radar over a sufficiently wide angle such that the scattering anisotropy may be detected. Fortunately, wide-angle SARs can illuminate targets over an aspect angle of $90°$, or even greater. It has recently been demonstrated [3] that a directional filter may be directly applied to the post-processed image to generate an image formed over any desired SAR subaperture. Although these filters were derived from first principles of backprojection in the spatial domain, their application may be more easily visualized in the spatial frequency domain.

Figure 2a) illustrates a SAR subaperture over an interval ϕ centered on look direction θ. The equivalent directional filter response is shown in Figure 2b). In the spatial frequency domain, the ideal directional filters form a segment of an annulus, where the orientation and angular span of the segment are determined by the look angle and subaperture interval, respectively. Moreover, temporal filtering may be embedded in the directional filter by varying the inner and outer radii of the annulus, which are directly proportional to the lower and upper cutoff frequencies of the filter. A sequence of N subaperture images, $I_{\theta_1},...,I_{\theta_N}$, may then be generated by filtering a post-processed image with a bank of directional filters, each designed with the appropriate direction θ.

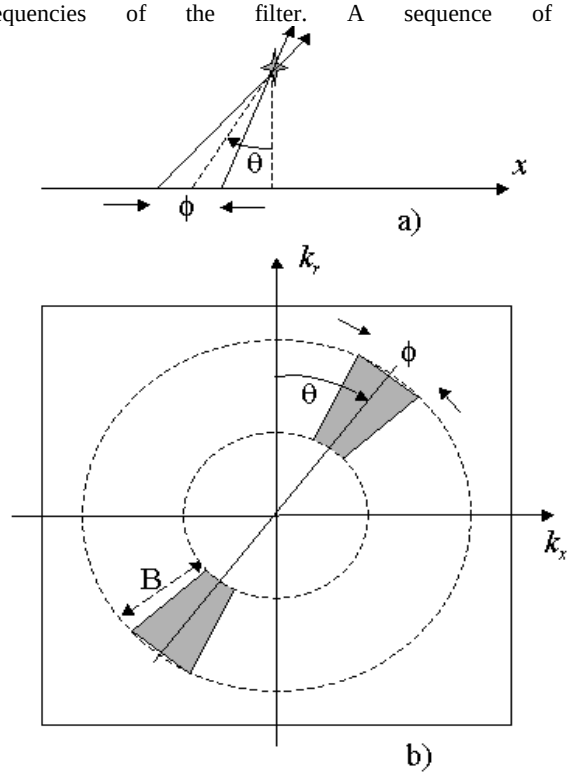

Figure 2. a) Generation of subaperture image with effective aperture ϕ from look direction θ relative to target. b) Response of the (ideal) equivalent directional filter in the spatial frequency domain, where B is the system bandwidth.

3. MATCHING PURSUITS FEATURE EXTRACTION

Given a sequence of subaperture images, we perform feature extraction on each image using the method of matching pursuits [4], a technique which iteratively decomposes any signal into a linear expansion of functions $e \in D$, where D is referred to as a "dictionary." The elements of the dictionary are designed to reflect the underlying structure present in the scattered signal, yielding a compact representation [7].

The matching pursuits decomposition is conducted as follows. For a given (subaperture) image, I_{θ_n}, the data is projected onto each element of the dictionary, and that element, e_1, for which the projection energy $|< I_{\theta_n}, e_1>|$ is maximized is selected. The image decomposition for the first iteration is then given by $< I_{\theta_n}, e_1> e_1$, and a remainder $R_1 = I_{\theta_n} - < I_{\theta_n}, e_1> e_1$ is defined. After N_i iterations, the decomposition is given by

$$I = \sum_{i=1}^{N_i} < R_{i-1}, e_i > e_i + R_{Ni} \qquad (1)$$

where $R_0 \equiv I$. After a sufficient number of iterations, the features may be defined as the parameters (or subset thereof) of the selected e_i, which represent the characteristics of scattering centers in the image. Such features may include amplitude, spatial extent in downrange and crossrange, and the frequency of resonances present in the imagery. Since each subaperture image is parameterized by a set of features, **y**, the *sequence* of subaperture images is described as a sequence of feature vectors $\boldsymbol{Y} = \mathbf{y}_1,\ldots,\mathbf{y}_N$. For the current application, the dictionary was developed using two-dimensional separable functions. Gabor functions [8] were utilized in the downrange direction, and a Hamming window, W_H, was employed in the crossrange. The dictionary was thus parameterized by the nominal scattering center location (x_0,r_0), center frequency (k), downrange extent (j), and crossrange extent (l):

$$e(x,r) = W_H(x - x_0, l)\cos(kr - \zeta)\exp(-\frac{(r - r_0)^2}{2^j}) \qquad (2)$$

Such a family of functions accounts for scattered signals representative of both wavefronts (small time support and large frequency support), and resonances (large time support and small frequency support). Appropriate crossrange window sizes may be determined by the resolution resulting from imaging over the SAR subaperture ϕ.

4. HMM DESIGN

Classification of targets exhibiting anisotropic scattering may be facilitated through the design of directionally dependent signal models. Wave scattering from most targets may be characterized

by angular sectors over which the scattering is relatively isotropic within each sector. Here we refer to such sectors as "states", with the number of states and the extent of each being characteristic of a given target. Generally, highly anisotropic targets will be described by several states encompassing the target, while simple targets, such as those exhibiting cylindrical symmetry, may be described using a single state. For a given target, T_m, the feature statistics within any given state, S_k, are considered to be stationary, and are described by the conditional density function $P(\mathbf{y} \mid S_i, T_m)$, which, in practice, is estimated from training data.

In this multi-aspect classification approach, the N subaperture images sample N discrete (but not necessarily distinct) states, $\boldsymbol{S} = S_1,\ldots,S_N$, characteristic of the target under interrogation. Since the states for a given target are fixed (and are determined by the scattering physics), the probability of transitioning from one state to another between consecutive subaperture images is dictated by the spatial extent of the state and the relative change in the target-sensor orientation. If we assume that the probability of making a state transition is governed only by the current state occupied, then the state sequence, $\boldsymbol{S}$, may be described as a discrete Markov chain [9]. Since the orientation of the target is assumed to be unknown, it follows that the state sequence $\boldsymbol{S}$ is unknown, and its identity may only be established through observation of the feature vector sequence $\boldsymbol{Y}$. We use HMMs [5] to model the statistics of the observed sequence $\boldsymbol{Y}$, which are driven by the underlying state sequence $\boldsymbol{S}$.

The use of discrete HMMs for single feature "flash" detection has been previously investigated [10]. Here we employ continuous mixture densities [11] to represent $P(\mathbf{y} \mid S_k, T_m)$, which overcomes common problems associated with quantization noise and limited training data. Furthermore, by using features associated with multiple physical attributes of the scattered signal, the anisotropy of the joint statistics of such features may be employed in target identification across several states, rather than relying solely on detecting an amplitude flash in a single state.

A continuous K-state HMM is represented by an initial state distribution K-vector, π, and K x K state-transition matrix, $\mathbf{A}$, with element a_{ij} being the probability of transitioning from state i to state j. The model also incorporates the observation densities for each state, $P(\mathbf{y} \mid S_k, T_m)$. Assume that the associated target may be represented by contiguous states with consecutive angular support $\psi_1,\ldots,\psi_K$. If the target orientation is uniformly distributed, then the probability that the first subaperture image was observed in state k is simply the proportion of that state's angular extent to the extent of all states, $\pi_k = \psi_k / \Sigma\psi_k$. Similarly, geometric considerations may be employed to determine the state transition probabilities, $\mathbf{A}$. For example, it is easily shown that if the angular target-sensor motion between consecutive subaperture images is smaller than the smallest state extent, $\psi_{\min}$, then transitions may only be made between adjacent states, resulting in non-zero elements of $\mathbf{A}$ only along the diagonal and sub-diagonal, given that the direction of motion (left-to right or right-to left) is known.

Given an observed sequence, $\boldsymbol{Y}$, and a set of target-specific HMMs, $\mathbf{M}_1,\ldots,\mathbf{M}_M$, the task of the HMM classifier is to determine which model was most likely to have produced $\boldsymbol{Y}$, *i.e.* we maximize $P(\boldsymbol{Y} \mid \mathbf{M}_m)$ over m. For a particular state sequence, $S_1,\ldots S_N$, the conditional probability of observing $\boldsymbol{Y}$, is given by

$$P(\boldsymbol{Y} \mid \boldsymbol{S},\mathbf{M}) = P(\mathbf{y}_1 \mid S_1,\mathbf{M})\, P(\mathbf{y}_2 \mid S_2,\mathbf{M}) \ldots P(\mathbf{y}_N \mid S_N,\mathbf{M}) \quad (3)$$

Therefore, the desired conditional likelihood may be computed by summing over all possible state sequences:

$$P(\boldsymbol{Y} \mid \mathbf{M}) = \sum_{\text{all } \boldsymbol{S}} P(\boldsymbol{Y} \mid \boldsymbol{S}, \mathbf{M}) P(\boldsymbol{S} \mid \mathbf{M}) \quad (4)$$

with the conditional state sequence given by the product of the transition probabilities with the initial state probability

$$P(\boldsymbol{S} \mid \mathbf{M}) = \pi_{S_1} a_{S_1 S_2} \ldots a_{S_{N-1} S_N} \quad (5)$$

The quantity in (4) may be efficiently computed via the forward-backward algorithm [12]. Alternatively, we employ the Viterbi algorithm [13] to estimate the maximum likelihood state sequence, which is subsequently used to calculate the likelihood of $\boldsymbol{Y}$. A Viterbi-based re-estimation procedure is used to optimize the model parameters according to training data.

5. APPLICATION TO SAR IMAGERY

In this section we present results from applying the multi-aspect HMM classification on data collected with the ARL BoomSAR [1], which operates in the frequency range 40-1200 MHz. The post-processed images were formed using standard backprojection methods over a 90° integration angle. Image "chips" containing tactical targets were selected and directionally filtered to generate a sequence of subaperture images. An example image chip of a target is shown in Figure 3a).

For this investigation the extent of the subaperture was fixed at $\phi = 6°$ with a look angle, θ, varying from -42° to 42° in 3° increments. Figure 3b) illustrates subaperture images generated for three look directions corresponding to a left, center and right aspect. Three iterations of the matching pursuits decomposition were performed on each of the subaperture images using the 2D dictionary described in Section 3, with the reconstruction associated with each subaperture shown in Figure 3b). For this study, three target chips were selected along with two clutter chips containing trees.

The hidden Markov models were trained using features from 10 subaperture images, with each *sequence* spanning 27°. Testing was performed using features extracted from a sequence of 10 subaperture images which were offset from the training subapertures by 1 degree, such that the training and testing data would be distinct. The discrimination power of the target models are shown in Figure 4, where the likelihood of observing feature sequences from each of the three targets and two clutter regions is computed from the model corresponding to target 1. It is seen that for all sequences of length 10 with initial subaperture look from -41° to 13°, that the likelihood of target 1 was greatest. Similar results were observed for HMMs designed for other targets. This performance is indicative of the promise that multi-aspect classification of SAR imagery holds.

To fully realize the potential of this target identification approach, electromagnetic scattering models of tactical targets

are being developed [6], enabling the scattered signal to be characterized at any orientation in the absence of system noise, and confounding clutter. Such models provide scattering data from all target states, which is difficult to ensure with measured data. Moreover, a complete state description will allow us to develop HMMs over subaperture sequences spanning the entire SAR aperture of 90°, enabling maximum exploitation of any anisotropy exhibited by the features. We are also investigating other methods of feature extraction, including the implementation of sub-bands within the directional filters which may be used to develop spectral as well as directionally dependent features.

a)

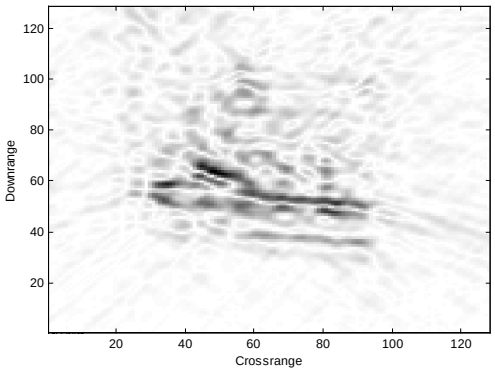

b)

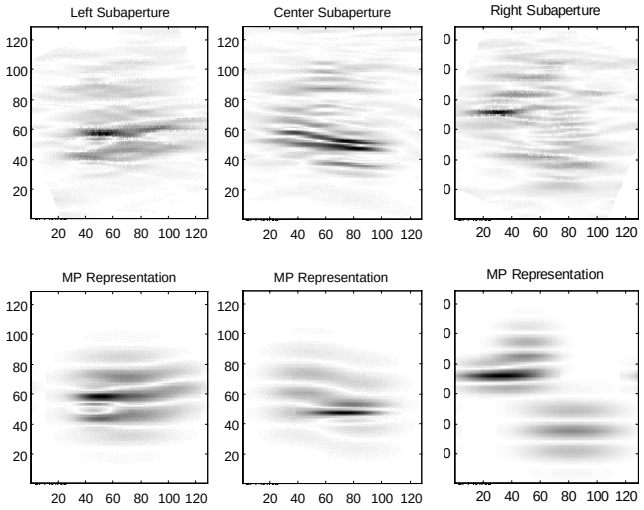

Figure 3. a) Image chip of target b) Top row - subaperture images: left (-24°), center (0°), right (24°); Bottom row – matching pursuits representation.

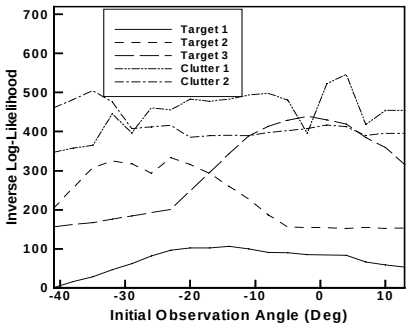

Figure 4. Inverse log-likelihood of feature sequences evaluated using HMM corresponding to target 1.

6. REFERENCES

[1] L. Nguyen et al., 'Ultra-wideband radar target discrimination using an advanced feature set," *Proceedings of SPIE, Detection and Remediation Technologies for Mine and Minelike Targets III*, April 1998.

[2] R. Kapoor et al., "Features for detecting obscured objects in ultra-wideband (UWB) SAR imagery using a phenomenological approach," Pattern Recognition, vol. 29, pp. 1761-1774, 1996.

[3] R. Rau and J.H. McClellan., "A directional image decomposition for ultra-wideband SAR". *IEEE International Conference on Acoustics, Speech, and Signal Processing*, 5:2877-2880 Seattle, 1997

[4] S.G. Mallat and Z. Zhang, "Matching pursuits with time-frequency dictionaries," *IEEE Trans. Sig. Proc.*, vol. 41, pp. 3397-3415, Dec. 1993.

[5] L.R. Rabiner, "A tutorial on hidden Markov models and selected applications in speech recognition," *Proc. IEEE*. vol.77, pp. 257-285, Feb. 1989.

[6] L.B. Felsen and N. Marcuvitz, *Radiation and Scattering of Waves*, Prentice-Hall Englewood-Cliffs, N.J., 1972.

[7] M. McClure and L. Carin, "Matching pursuits with a wave-based dictionary," *IEEE Trans. Sig. Proc.*, vol. 45, pp. 2912-2927, Dec. 1997.

[8] C.S. Burrus, R.A. Gopinath, H. Guo, *Introduction to Wavelets and Wavelet Transforms*, Prentice-Hall, Englewood Cliffs, N.J., 1997

[9] A. Papoulis, *Probability random Variables and Stochastic Processes*, 3rd edition, McGraw-Hill, New York, 1991.

[10] L.R. Flake et al., "Detecting anisotropic scattering with hidden Markov models," *IEE Proc. Radar, sonar, Navig.*, vol. 144, pp. 81-86, April, 1997

[11] L.R. Rabiner et al., "Some properties of continuous hidden Markov Model representations," *AT&T Tech. J.* vol. 64 pp1251-1269, July 1985.

[12] L.E. Baum et al., " A Maximization technique occurring in the statistical analysis of Markov chains," *Ann. Math. Stat.*, vol. 41, pp. 164-171, 1973

[13] A. Viterbi, "Error bounds for convolutional codes and an asymptotically optimum decoding algorithm," *IEEE Trans. Inform, Theory*, vol. 13, pp. 260-269, April 1967.